

# Peristaltic Transport of a Conducting Bingham Fluid in an Inclined Channel with Permeable Walls by Adomian Decomposition Method

Rathod.V.P and Laxmi Devindrappa

Department of studies and Research in Mathematics, Gulbarga University,  
Gulbarga-585106, Karnataka, India

**ABSTRACT** *In this paper, Peristaltic transport of a conducting Bingham fluid in an inclined channel with permeable walls by Adomian decomposition method has been studied. The flow is examined in a wave frame of reference moving with the velocity of wave and the resulting equations have then been simplified using the assumptions of long wavelength and low Reynolds number approximation. The effects of various parameters of interest on these formulas were discussed and illustrated graphically through a set of graphs. using the assumptions of long wavelength and low Reynolds number approximation. The effects of various parameters of interest on these formulas were discussed and illustrated graphically through a set of graphs.*

**Keywords-** *Adomian decomposition method, Peristaltic transport, friction force, Bingham fluid.*

## 1. INTRODUCTION

Peristalsis is now well known to physiologists to be one of the major mechanisms for fluid transport in many biological systems. Peristaltic pumping occurs in many practical applications involving biomedical systems. Many modern medical devices have been designed on the principle of peristaltic pumping to transport fluids without internal moving parts, for example, the blood in the heart-lung machine. The main motivation for any mathematical analysis of physiological fluid flows is to ultimately have a better understanding of the particular flow being modelled. If there is similarity between the results obtained from the analysis and experimental and clinical data, then the mechanism of flow can at least be explained. Because peristalsis is evident in many physiological flows, an accurate mathematical study can help explain the major contributing factors to many flows in the human body. When comparing results between the mathematical model and the experimental and clinical data, it

is desirable that the data obtained from experimental research be as close as possible to the actual physiological parameter being analysed. That is to say, it may be necessary to take into account the effect the measuring instrument or device or procedure has on the data obtained. The study of the mechanisms of peristalsis, in both mechanical and physiological situations, has become the subject of scientific research for quite some time. Since the first investigation of Latham [1], several theoretical and experimental attempts have been made to understand peristaltic action in different situations.

There are many types of non-Newtonian fluids: shearing thinning fluid, viscoplastic fluid and viscoelastic fluid. In this report, we will focus on the viscoplastic fluid. Viscoplastic fluid is also called "yield stress" fluid. Such fluid has a property in which the fluid behaves like a solid below some critical stress value (the yield stress), but flows like a viscous liquid when the yield stress is exceeded. It is often associated with highly aggregated suspensions. Flow of the muddy rivers is a typical example. Among many viscoplastic fluids, there is a special class called Bingham plastics. For Bingham plastic fluid, the shear stress beyond the yield stress is linearly proportional to the shear rate. If the yield stress approaches zero, the Bingham plastic fluid can be approximately treated as Newtonian fluid. Rathod and Laxmi [2] have studied the effects of heat transfer on the peristaltic MHD flow of a Bingham fluid through a porous medium in a channel.

If a magnetic field is applied to a moving electrically conducting liquid, it induces electric and magnetic fields. The interaction of these fields produces a body force known as Lorentz force which has a tendency to oppose the movement of the liquid [3]. Stud *et al.* [4] studied the effect of moving magnetic field on blood flow and observed that the effect of suitable moving magnetic field accelerates the speed of blood. Rathod *et al.* [5-27] made a

detailed study on peristaltic transport in Newtonian or non-Newtonian fluid.

In this paper Peristaltic transport of a conducting Bingham fluid in an inclined channel with permeable walls by Adomian decomposition method is investigated under long wavelength and low Reynolds number assumptions. The effects of various emerging parameters on the flow, temperature, concentration distributions are discussed with the help of graphs.

## II. MATHEMATICAL FORMULATION

Consider the peristaltic pumping of a conducting Bingham fluid in a channel with permeable walls, under long wavelength and low Reynolds number assumptions. The flow in a channel is governed by Navier-stokes equations whereas the flow in the wall is described by Darcy's law. The channel is of half-width  $a$ . A longitudinal train of progressive sinusoidal waves takes place on the upper and lower walls of the channel. For simplicity, we restrict our discussion to the half-width  $a$  of the channel as shown in the figure. The channel is inclined at an angle  $\theta$  with the horizontal. The region between  $y = 0$  and  $y = y_0$  is called plug flow region. In the plug flow region  $|\tau_{yx}| \leq \tau_0$ . In the region between  $y = y_0$  and  $y = H$ ,  $|\tau_{yx}| > \tau_0$ . The wall deformation is given by

$$H(X, t) = a + b \sin \frac{2\pi}{\lambda} (x - ct) \quad (2.1)$$

where  $b$  is the amplitude,  $\lambda$  the wavelength and  $c$  is the wave speed. Under the assumptions that the channel length is an integral multiple of the wavelength  $\lambda$  and the pressure difference across the ends of the channel is a constant, the flow becomes steady in the wave frame  $(x, y)$  moving with velocity  $c$  away from the fixed (laboratory) frame  $(X, Y)$ . The transformation between these two frames is given by

$$\begin{aligned} x &= X - ct, y = Y, u(x, y) = U(X - ct, Y) \\ \text{and } v(x, y) &= V(X - ct, Y) \end{aligned} \quad (2.2)$$

Where  $U$  and  $V$  are velocity components in the laboratory frame and  $u$  and  $v$  are velocity components in the wave frame. In the many physiological situations it is proved experimentally that the Reynolds number of the flow is very small. So, we assume that the wavelength is infinite. So the flow is of Poiseuille type at each local cross - section.

Under these assumptions the governing equations of the flow are

$$\frac{\partial u}{\partial y} \left( \tau_0 - \mu \frac{\partial u}{\partial y} \right) + \sigma B_0^2 u = -\frac{\partial p}{\partial x} - \eta_1 \sin \theta \quad (2.3)$$

$$0 = -\frac{\partial p}{\partial y} + \eta_2 \cos \theta \quad (2.4)$$

Introducing the non-dimensional quantities

$$\begin{aligned} x &= \frac{x}{\lambda}, y = \frac{y}{a}, u = \frac{u}{c}, p = \frac{pa^2}{\mu c \lambda}, \\ t &= \frac{ct}{\lambda}, h = \frac{H}{a}, \phi = \frac{b}{a}, \tau_0 = \frac{a\tau_0}{\lambda}, \\ y_0 &= \frac{y_0}{a}, M = \sqrt{\frac{\rho}{\mu}} a B_0, \text{Re} = \frac{\rho c a}{\mu}, \\ Da &= \frac{k}{a^2} \end{aligned}$$

We introduce the stream function  $\psi$  such that

$$u = \frac{\partial \psi}{\partial y}, v = -\frac{\partial \psi}{\partial x}$$

After non-dimensionalisation (after dropping bars)

$$\frac{\partial u}{\partial y} \left( \tau_0 - \psi_{yy} \right) + M^2 \psi_y = -\frac{\partial p}{\partial x} - \eta_1 \sin \theta \quad (2.5)$$

$$0 = -\frac{\partial p}{\partial y} \tag{2.6}$$

where  $\eta_1 = \frac{p g a^2}{\mu c}$  and  $\eta_2 = \frac{p g a^3}{\mu c \lambda}$  and  $g$  is the acceleration due to gravity

The non-dimensional boundary conditions are

$$\frac{\partial u}{\partial y} = \tau_0 \text{ at } y = 0 \tag{2.7}$$

$$u = -1 - \frac{\sqrt{Da}}{\alpha} \frac{\partial u}{\partial y} \text{ at } y = h \tag{2.8}$$

Where  $\psi$  is the stream function,  $\alpha$  is slip parameter and  $\tau_0$  is the yield stress.

The volume flux  $q$  through each cross section in the wave frame is given by

$$q = \int_0^{y_0} u_p dy + \int_{y_0}^h u dy \tag{2.9}$$

The instantaneous volume flow rate  $Q(X, t)$  in the laboratory frame between the centre line and the wall is

$$Q(X, t) = \int_0^H U dy = \int_0^h (u + 1) dy = q + h \tag{2.10}$$

### III. METHOD OF SOLUTION

Solving equation (2.5) and (2.6) subject to the boundary conditions (2.7) and (2.8) by using the Adomian decomposition method we obtain the velocity as

$$u = -\frac{\frac{dp}{dx} \left( \alpha \text{Cosh}[hM] - \alpha \text{Cosh}[M y] \right)}{M^2 \left( \alpha \text{Cosh}[hM] + \sqrt{Da} M \text{Sinh}[hM] \right)} \frac{\left( \begin{aligned} &\sqrt{Da} M^2 \tau_0 \text{Cosh}[M(h-y)] \\ &+ M^2 \alpha \text{Cosh}[M y] - \alpha \eta_1 \\ &\text{Cosh}[M h] \text{Sin}[\theta] + \\ &\alpha \eta_1 \text{Cosh}[M y] \text{Sin}[\theta] - \\ &\sqrt{Da} M \eta_1 \text{Sinh}[M h] \text{Sin}[\theta] + \\ &\alpha \tau_0 M \text{Sinh}[M(h-y)] \end{aligned} \right)}{M^2 \left( \alpha \text{Cosh}[hM] + \sqrt{Da} M \text{Sinh}[hM] \right)} \tag{3.1}$$

Taking  $y = y_0$  in equation (3.1), we get the velocity in the plug flow region as

$$u_p = -\frac{\frac{dp}{dx} A_1}{A_3} - \frac{A_2}{A_3}$$

The volume flux  $q$  through each cross section in the wave frame is given by

$$q = \int_0^{y_0} u_p dy + \int_{y_0}^h u dy = \frac{\left( \frac{dp}{dx} A_4 \right)}{A_5} - \frac{1}{A_5} (-A_6 - A_7 - A_8 + A_9) \tag{3.2}$$

Where

$$A_1 = \left( \left( \alpha \text{Cosh}[hM] - \alpha \text{Cosh}[M y_0] \right) \right) \left( \frac{1}{\alpha \text{Cosh}[hM] + \sqrt{Da} M \text{Sinh}[hM]} \right)$$

$$\begin{aligned} A_2 &= \sqrt{Da} M^2 \tau_0 \text{Cosh}[M(h-y_0)] \\ &+ M^2 \alpha \text{Cosh}[M y_0] - \alpha \eta_1 \text{Cosh}[M h] \\ &\text{Sin}[\theta] + \alpha \eta_1 \text{Cosh}[M y_0] \text{Sin}[\theta] - \\ &\sqrt{Da} M \eta_1 \text{Sinh}[M h] \text{Sin}[\theta] + \\ &\alpha \tau_0 M \text{Sinh}[M(h-y_0)] \end{aligned}$$

$$A_3 = M^2 \left( \begin{array}{c} \alpha \text{Cosh}[hM] + \\ \sqrt{Da} M \text{Sinh}[hM] \end{array} \right)$$

$$A_4 = \left( \begin{array}{c} hM \alpha \text{Cosh}[hM] + \sqrt{Da} hM^2 \\ \text{Sinh}[hM] - \alpha \text{Sinh}[hM] + \alpha \\ \text{Sinh}[My_0] - M \alpha \text{Cosh}[My_0] y_0 \end{array} \right)$$

$$A_5 = \left( M^3 \left( \begin{array}{c} \alpha \text{Cosh}[hM] + \sqrt{Da} \\ M \text{Sinh}[hM] \end{array} \right) \right)$$

$$A_6 = M \alpha \tau + M \alpha \tau \text{Cosh} \\ [M(h - y_0)] - hM \alpha \eta \text{Cosh}[hM] \\ \text{Sin}[\theta] + M^2 \alpha \text{Sinh}[hM]$$

$$A_7 = \sqrt{Da} hM^2 \eta \text{Sin}[\theta] \text{Sinh}[hM] \\ + \alpha \eta \text{Sin}[\theta] \text{Sinh}[hM] \\ + \sqrt{Da} M^2 \tau \text{Sinh}[M(h - y_0)]$$

$$A_8 = M^2 \alpha \text{Sinh}[My_0] - \alpha \eta \\ \text{Sin}[\theta] \text{Sinh}[My_0] + \sqrt{Da} M^3 \\ \tau \text{Cosh}[M(h - y_0)] y_0$$

$$A_9 = M^3 \alpha \text{Cosh}[My_0] y_0 + \\ M \alpha \eta \text{Sin}[\theta] \text{Cosh}[My_0] y_0 \\ + M^2 \tau \alpha \text{Cosh}[M(h - y_0)] y_0$$

From Eq. (3.2) we have

$$\frac{dp}{dx} = \frac{A_5 (q + (-A_6 - A_7 - A_8 + A_9))}{A_4} \quad (3.3)$$

The pressure rise and frictional force over one wavelength of the peristaltic are given by

$$\Delta p = \int_0^1 \frac{dp}{dx} dx \quad (3.4)$$

$$F = \int_0^1 h \left( -\frac{dp}{dx} \right) dx \quad (3.5)$$

The above integrals numerically evaluated using the MATHEMATICA software.

#### IV. RESULTS AND DISCUSSION

In this section, numerical results of the problem under discussion are discussed through graphs. Numerical simulation is performed using the computational software Mathematica.

(Figs. 2-7) illustrate the variations of  $\frac{dp}{dx}$  for a

given wavelength versus x. (Fig. 2) shows the small amount of pressure gradient is required to pass the flow in the wider part of the channel in an asymmetric channel when compared to the symmetric channel for different values of  $\phi$

$$d = 2, M = 3, D_a = 0.01, a = 0.7,$$

with

$$R_e = 10, F_r = 2, \alpha = \frac{\pi}{4} \text{ and } b = 1.2$$

(Fig. 3) shows the magnitude of pressure gradient increases by increasing the Hartmann number  $M$  with

$$d = 2, \phi = \frac{\pi}{6}, D_a = 0.1, a = 0.7, R_e = 10,$$

$$F_r = 2, \alpha = \frac{\pi}{4} \text{ and } b = 1.2$$

(Fig. 4) shows the variation of pressure gradient  $\frac{dp}{dx}$  with Darcy number  $D_a$  for

$$d = 2, \phi = \frac{\pi}{6}, M = 3, a = 0.7, R_e = 10,$$

$$F_r = 2, \alpha = \frac{\pi}{4} \text{ and } b = 1.2$$

is found that, by increasing the Darcy number  $D_a$  decreases the axial pressure gradient. (Fig. 5) shows the variation of pressure gradient for different values of inclination angel  $\alpha$

$$d = 2, \phi = \frac{\pi}{6}, M = 3, D_a = 0.001,$$

$$a = 0.7, R_e = 10, F_r = 2 \text{ and } b = 1.2$$

is found that, increasing the  $\alpha$  increases the axial pressure gradient. (Fig. 6) shows the magnitude of pressure gradient decreases by increasing the Froude number  $F_r$  with

$$d = 2, M = 3, \phi = \frac{\pi}{6}, D_a = 0.001,$$

$$a = 0.7, R_e = 10, \alpha = \frac{\pi}{4} \text{ and } b = 1.2$$

(Fig. 7) it is found that, pressure gradient increases with increasing  $R_e$  with

$$d = 2, M = 3, \phi = \frac{\pi}{6}, D_a = 0.001,$$

$$a = 0.7, F_r = 2, \alpha = \frac{\pi}{4} \text{ and } b = 1.2$$

(Fig. 8-11) shows the variation of temperature profile for different values of Hartmann number  $M$ , Darcy number  $Da$ , Prandtl number  $p_r$ , Eckert number  $E_c$ , Schmidt number  $S_c$ , Soret number  $S_r$  and Dufour number  $D_f$ . From (Fig. 9-11) it is clear that by increasing  $Da$ ,  $p_r$  and  $E_c$  the temperature profile increases, while from Figure 8 we observe that the temperature profile decreases with the increase in  $M$ .

(Fig. 12-18) are plotted to study the effects of  $M$ ,  $Da$ ,  $p_r$ ,  $E_c$ ,  $S_r$ ,  $S_c$  and  $D_f$  on the concentration profile. (Fig. 12) illustrates that by increasing  $M$  the concentration profile increase. (Fig. 13-15) shows that concentration profile decreases with the increase in  $Da$ ,  $p_r$  and  $E_c$ . It is also seen from (Fig. 16) that with an increase in Schmidt number  $S_c$  and Soret number  $S_r$ , the concentration decreases.

The values of  $S_r$  and  $D_f$  are chosen in such way that their product is a constant value, since the mean temperature is kept constant. (Fig. 17) shows that by decreasing  $D_f$  and increasing  $S_r$  the concentration profile decreases, while from (Fig. 18) it is clear that by increasing  $D_f$  and decreasing  $S_r$  the concentration profile increases.

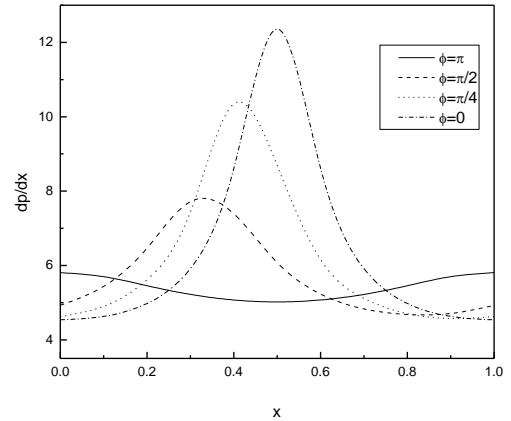


Fig. 2. Pressure gradient versus  $x$  for

$$d = 2, \alpha = \frac{\pi}{4}, M = 3, D_a = 0.01, a = 0.7, R_e = 10, F_r = 2 \text{ and } b = 1.2$$

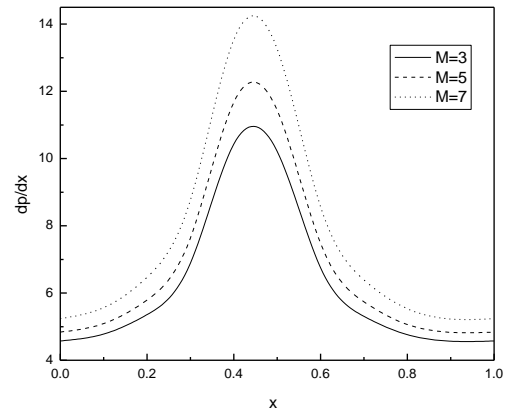


Fig. 3. Pressure gradient versus  $x$  for

$$d = 2, \alpha = \frac{\pi}{4}, \phi = \frac{\pi}{6}, D_a = 0.1, a = 0.7, R_e = 10, F_r = 2 \text{ and } b = 1.2$$

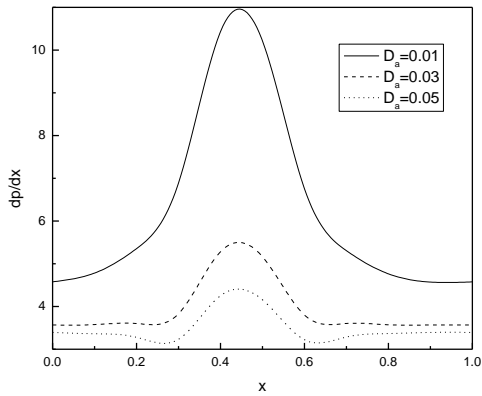


Fig. 4. Pressure gradient versus  $x$  for

$$d = 2, \alpha = \frac{\pi}{4}, M = 3, \phi = \frac{\pi}{6}, a = 0.7, R_e = 10, F_r = 2 \text{ and } b = 1.2$$

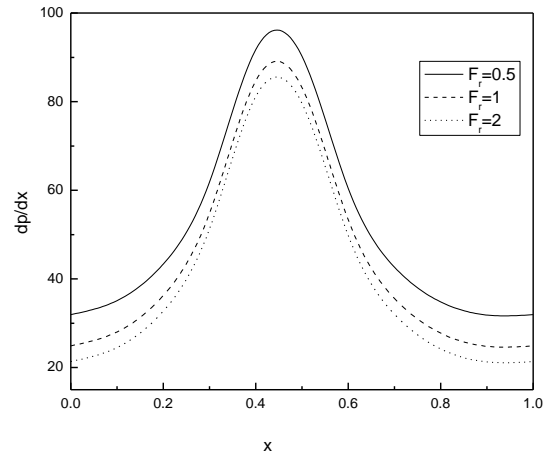


Fig. 6. Pressure gradient versus  $x$  for

$$d = 2, \alpha = \frac{\pi}{4}, a = 0.7, R_e = 10, \phi = \frac{\pi}{6}, M = 3, D_a = 0.001, \text{ and } b = 1.2$$

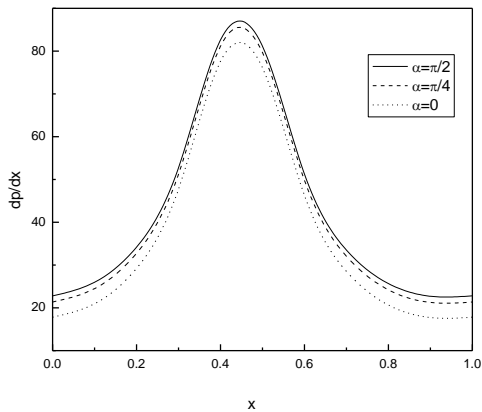


Fig. 5. Pressure gradient versus  $x$  for

$$d = 2, \phi = \frac{\pi}{6}, M = 3, D_a = 0.001, a = 0.7, R_e = 10, F_r = 2 \text{ and } b = 1.2$$

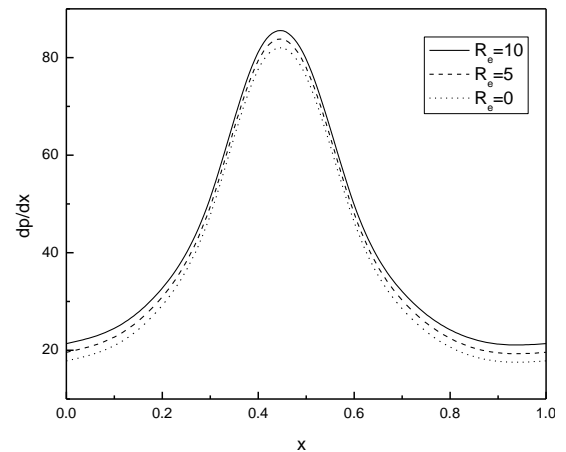


Fig. 7. Pressure gradient versus  $x$  for

$$d = 2, \alpha = \frac{\pi}{4}, a = 0.7, F_r = 2, \phi = \frac{\pi}{6}, M = 3, D_a = 0.001, \text{ and } b = 1.2$$

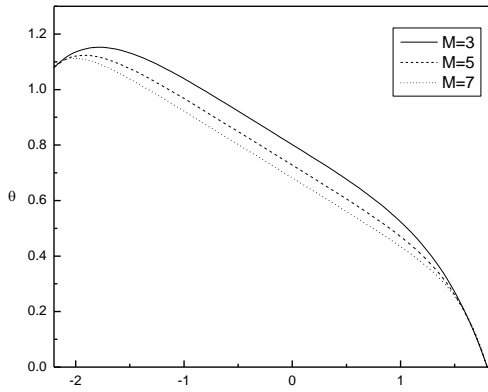


Fig. 8. Temperature profile for

$$d = 1.5, a = 0.8, \phi = \frac{\pi}{4}, d_r = 0.1, \\ p_r = 2, D_a = 2, E_c = 0.5, S_r = 0.6, \\ S_c = 0.5 \text{ and } b = 1.2$$

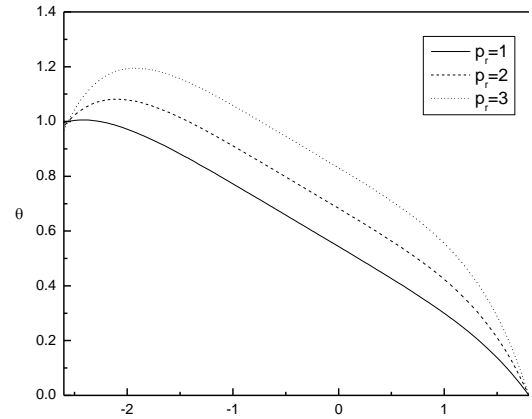


Fig. 10. Temperature profile for

$$d = 1.5, a = 0.8, \phi = \frac{\pi}{4}, d_r = 0.1, M = 3, D_a = 2, \\ E_c = 0.5, S_r = 0.6, S_c = 0.5 \text{ and } b = 1.5$$

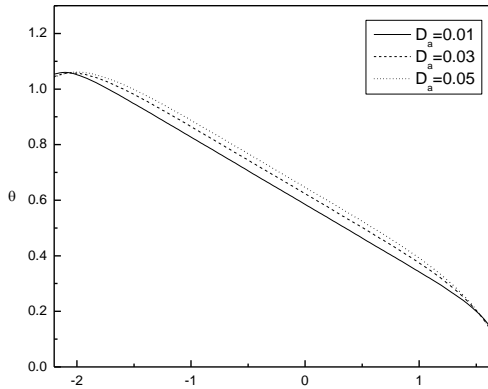


Fig. 9. Temperature profile for

$$d = 1.5, a = 0.8, \phi = \frac{\pi}{8}, d_r = 0.1, \\ p_r = 2, M = 2, E_c = 0.5, S_r = 0.6, \\ S_c = 0.5 \text{ and } b = 0.9$$

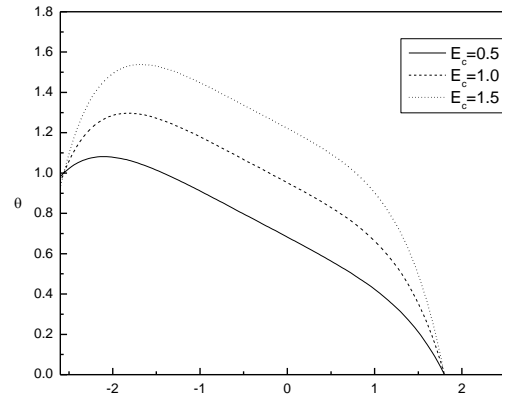


Fig. 11. Temperature profile for

$$d = 1.5, a = 0.8, \phi = \frac{\pi}{4}, d_r = 0.1, p_r = 2, D_a = 2, \\ M = 3, S_r = 0.6, S_c = 0.5 \text{ and } b = 1.5$$

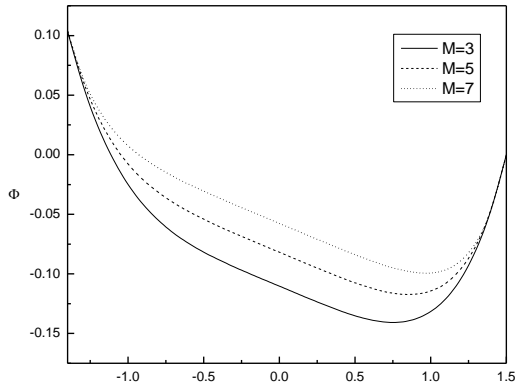


Fig. 12. Concentration profile for

$$d = 1.5, a = 0.5, \phi = \frac{\pi}{2}, d_r = 0.1,$$

$$p_r = 3, D_a = 2, E_c = 0.8, S_r = 0.7,$$

$$S_c = 0.6 \text{ and } b = 1.2$$

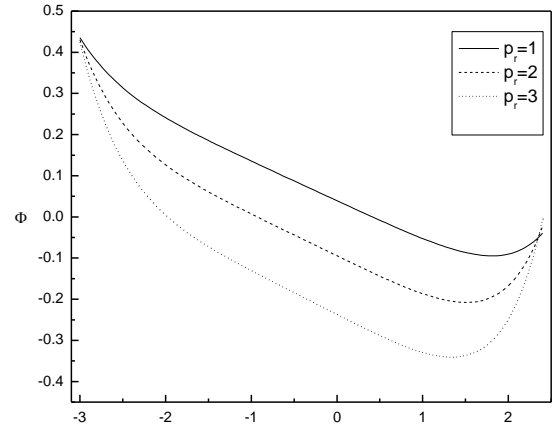


Fig. 14. Concentration profile for

$$d = 1.5, a = 0.5, \phi = \frac{\pi}{4}, d_r = 0.1, D_a = 2, M = 3,$$

$$E_c = 0.5, S_r = 0.6, S_c = 0.5 \text{ and } b = 1.2$$

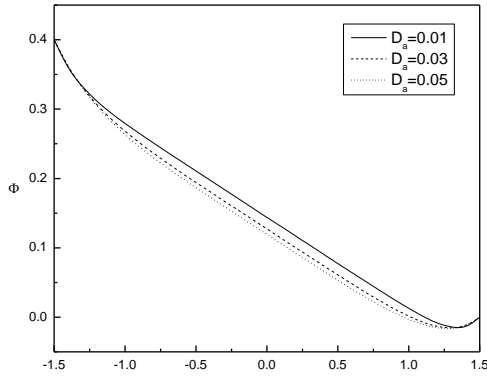


Fig. 13. Concentration profile for

$$d = 1.5, a = 0.5, \phi = \frac{\pi}{2}, d_r = 0.1,$$

$$p_r = 2, M = 2, E_c = 0.5, S_r = 0.6,$$

$$S_c = 0.5 \text{ and } b = 1.2$$

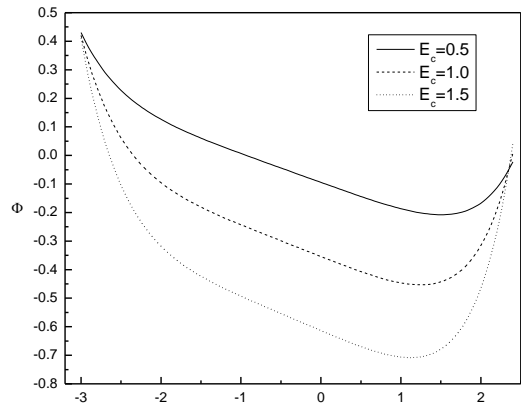


Fig. 15. Concentration profile for

$$d = 1.5, a = 0.8, \phi = \frac{\pi}{4}, d_r = 0.1, p_r = 2, M = 3,$$

$$D_a = 2, S_r = 0.6, S_c = 0.5 \text{ and } b = 1.5$$



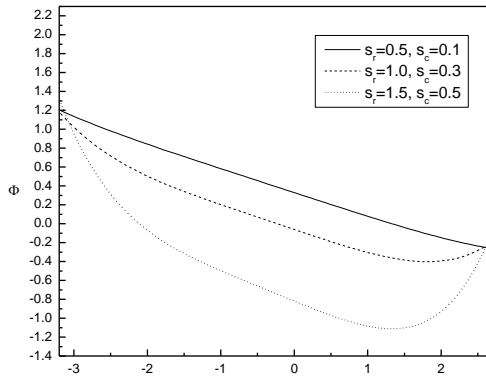


Fig. 16. Concentration profile for

$$d = 1.5, a = 0.6, \phi = \frac{\pi}{4}, d_r = 0.1, p_r = 2, M = 1, \\ E_c = 0.5, D_a = 2 \text{ and } b = 1.2$$

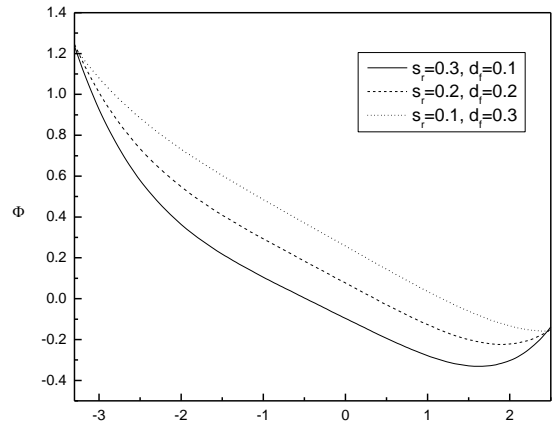


Fig. 18. Concentration profile for

$$d = 1.5, a = 0.8, \phi = \frac{\pi}{4}, p_r = 2, M = 1, \\ E_c = 0.5, D_a = 2, S_c = 1 \text{ and } b = 1.2$$

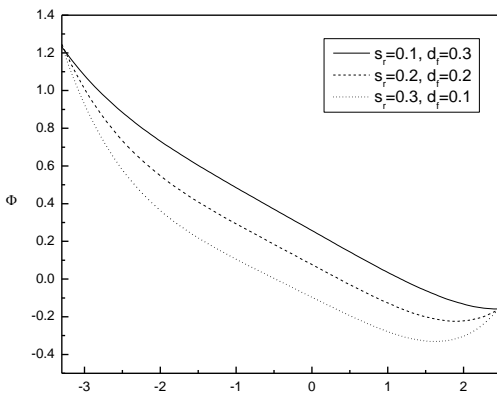


Fig. 17. Concentration profile for

$$d = 1.5, a = 0.8, \phi = \frac{\pi}{4}, s_c = 1, p_r = 2, M = 1, \\ E_c = 0.5, D_a = 1 \text{ and } b = 1.2$$

## V. CONCLUSIONS

In the present study we conclude with the observations as, In the center of the channel, the pressure gradient increases with an increase in  $M, \alpha, R_e$ . However it decreases with an increase in  $D_a, F_r$  and  $\phi$ . The temperature profile increases with the increase in  $Da, p_r$  and  $E_c$  and decreases with an increase in  $M$ . The concentration profile decrease with the increase in  $Da, p_r$  and  $E_c$ . It is observed with an increase in Schmidt number  $S_c$  and Soret number  $S_r$ , the concentration profile decreases. The concentration profile decreases by decreasing  $D_f$  and increasing  $S_r$ . It is clear that by increasing  $D_f$  and decreasing  $S_r$  the concentration profile increases.

## ACKNOWLEDGMENTS

This work is supported by UGC, Research Fellowship in Science for Meritorious Students (RFSMS) [void UGC Ltr. No.F.No. 7-72/2007(BSR) date 10.01.2012]. One of the authors, Ms. Laxmi Devindrappa, acknowledges UGC for awarding the Research Fellowship.

## REFERENCES

- [1] T.W. Latham, Fluid motion in a peristaltic pump, *MS. Thesis, Massachusetts Institute of Technology, Cambridge, MA.* (1966).
- [2] V. P. Rathod and Laxmi Devindrappa, effects of heat transfer on the peristaltic MHD flow of a Bingham fluid through a porous medium in a channel, *Int. J. Biomathematics.* 7, 1450060-20, (2014).
- [3] I. J. D. Craig and P. G. Watson, Magnetic reconnection solutions based on a generalized Ohm's law, *Solar Physics.* 214, 131-150, (2003).
- [4] V. K. Stud, G. S. Sephon and R. K. Mishra, Pumping action on blood flow by a magnetic field, *Bull. Math. Biol.* 39, 385, (1977).
- [5] V. P. Rathod and S. K. Asha, Peristaltic transport of a couple stress fluid in a uniform and non uniform annulus, *International journal of mathematical modeling, simulation and application.* 2, 414-426, (2009).
- [6] V. P. Rathod and S. K. Asha, Effect of couple stress fluid and an endoscope in peristaltic motion, *Ultra Science.* 21, 83-90, (2009).
- [7] V. P. Rathod and S. K. Asha, Effects of magnetic field and an endoscope on peristaltic motion, *Advance in applied science research.* 2, 102-109, (2012).
- [8] V. P. Rathod and S. K. Asha, Peristaltic transport of a magnetic fluid in a uniform and non-uniform annulus, *International Journal of Mathematical Archive.* 3, 1-11, (2012).
- [9] V. P. Rathod and S. K. Asha, Effect of Couple Stress fluid on Peristaltic motion in a uniform and Non-uniform annulus, *International Journal of Computer and Organizations Trends.* 3, 109-117, (2013).
- [10] V. P. Rathod and S. K. Asha, Peristaltic transport of a couple stress fluid in a uniform and non uniform annulus, *Journal of Chemical, Biology and Physical Science.* 4, 468-480, (2014).
- [11] V.P. Rathod And M.M. Channakote, Effect of magnetic field on ureteral peristalsis in cylindrical tube, *Ultra Scientist of Physical Sciences.* 23, 135-142, (2011).
- [12] V.P. Rathod and M.M. Channakote, Effect of thickness of the porous material on the peristaltic pumping of a Jeffry fluid when the tube wall is provided with non- erodible porous lining, *International Journal of Mathematical Archive.* 2, 1-10, (2011).
- [13] V.P. Rathod and M.M. Channakote, A study of ureteral peristalsis with fluid flow, *International journal of Mathematical Modeling, Simulation and Application.* 5, 11-22, (2012).
- [14] V.P. Rathod and M.M. Channakote, Slip effects and heat transfer on MHD peristaltic flow of Jeffrey fluid in an inclined channel, *Journal of Chemical, Biological and Physical Sciences.* 2, 1987-97, (2012).
- [15] V.P. Rathod and M.M. Channakote, A Study of Ureteral Peristalsis in Cylindrical Tube through Porous Medium, *Advances in Applied Science Research.* 2, 134-140, (2011).
- [16] V.P. Rathod and M.M. Channakote, Interaction of heat transfer and peristaltic pumping of fractional second grade fluid through a vertical cylindrical tube, *Thermal science.* 18, 1109-1118, (2014).
- [17] V.P.Rathod and Pallavi Kulkarni, The influence of wall properties on MHD Peristaltic transport of dusty fluid, *Advances in Applied Science Research.* 2, 265-279, (2011).
- [18] V.P.Rathod and Pallavi Kulkarni, The influence of wall properties on Peristaltic transport of dusty fluid through porous medium, *International Journal of Mathematical Archive.* 2, 1-13, (2011).
- [19] V.P.Rathod and Pallavi Kulkarni, The effect of slip condition and heat transfer on MHD peristaltic transport through a porous medium with complaint wall. *Int.J.Applied Mathematical Sciences.* 5, 47-63, (2011).
- [20] V. P. Rathod and N. G. Sridhar, Peristaltic transport of couple stress fluid in uniform and non-uniform annulus through porous medium, *International Journal of Mathematical Archive.* 3, 1561-1574, (2012).
- [21] V. P. Rathod, N. G. Sridhar and M. Mahadev, Peristaltic pumping of couple stress fluid through non - erodible porous lining tube wall with thickness of porous material, *Advances in Applied Science Research.* 3, 2326-2336, (2012).
- [22] V. P. Rathod and N. G. Sridhar, Peristaltic flow of a couple stress fluids through a porous medium in an inclined channel, *Journal of Chemical, Biological and Physical Sciences.* 5, 1760-1770, (2015).
- [23] V. P. Rathod and Laxmi Devindrappa, Slip effect on peristaltic transport of a conducting fluid through a porous medium in an asymmetric vertical channel by adomian decomposition method, *International journal of mathematical archive.* 4, 133-141, (2013).
- [24] V. P. Rathod and Laxmi Devindrappa, Peristaltic transport of a conducting fluid in an asymmetric vertical channel with heat and mass transfer. *Journal of chemical, biological and physical sciences.* 4, 1452-1470, (2014).
- [25] V. P. Rathod and Laxmi Devindrappa, Effects of heat transfer on the peristaltic MHD flow of a Bingham Fluid through a porous medium in an inclined channel, *Mathematical sciences international research journal.* 3, (2014).
- [26] V. P. Rathod, Anita Tuljappa and Laxmi B, Effect of magnetic field on the peristaltic flow of a fractional second grade fluid through a cylindrical tube, *International journal of mathematical archive.* 6, 133-143, (2015).
- [27] V. P. Rathod and Anita Tuljappa, Peristaltic flow of a fractional second grade fluid through inclined cylindrical tube, *International journal of mathematical archive.* 6, 29-46, (2015).